

Response to referee O.P. Savchuk

We thank the referee for his rigorous and insightful comments on the manuscript. Our responses are listed below. Referee comments in italics.

Major concerns

1. *In the revised version, it became even clearer that the manuscript deals with a study of the model itself rather than with a usage of the model for studying the marine system. As the authors admitted: Much of the JUSTIFICATION certainly boils down to the USE of a relatively NEW TOOL. we feel that an ILLUSTRATION OF ITS USES is valuable. As deficit of geographical and biogeochemical plausibility cannot be compensated by methodological novelty of the implemented statistical tool (wavelet analysis), such study is more appropriate, perhaps, for the journals dealing with modelling technics rather than in Biogeosciences (see my initial comments).*

We understand the concerns put forward by both referees regarding the lack of comparison with real data. We have added references to studies that includes validation of nutrients, temperature and salinity for the particular model run used in our study. Validation of the different plankton species is difficult due to lack of observations and essentially unknown C:Chl ratio, and had not previously been done for the model run we use. We have now added such an evaluation of the biology, assuming a fixed C:Chl ratio of 50 shown in Fig. 3 and 4. The fixed ratio is likely responsible for part of the model-observation difference in absolute values, but has probably a negligible impact on the timing of blooms.

2. *The revisions concerning nutrient limitation are still confusing and misleading in respect to the real Baltic as we know it from both observations and simulations with other models. No consideration is given to how an appropriate re-parameterization of internally inconsistent N-limitation & P-limitation as determined by a specific set of constants prescribed in result of calibration of this specific model, while a sensitivity of simulation to such a choice is not even mentioned. The manuscript still contains a little addition in- , perhaps, even directly contradicts to existing knowledge about the relationships between nutrient and phytoplankton dynamics in the Baltic Proper. In that respect, particularly surprisingly and unconvincingly sound such expressions as a shift towards less limited conditions (Line223), Phosphate is still limiting during winter (L230), the phase shifts from NUTLIM preceding diatoms by three months to diatoms preceding nutlim by the same amount (L245-246) and the following considerations of maximal NUTLIM on Fig.11 (shouldnt minimum NUTLIM be more interesting?), The spring bloom is phosphate limited throughout*

the run except for a few years after 1990 where diatoms display nitrogen limitation (L304-305). Correspondingly, the entire Section 3.2, including Figs. 6-11 still looks just as exercise with a new tool, being more concerned with the tool rather than the Baltic. Perhaps, it can be focused only on analysis of N:P instead of NUTLIM and substantially shortened, absorbing and compressing much from the Summary and Conclusions Section as well.

As stated in our answers to the previous review comments, if NLIM is larger than one, PLIM is used. NUTLIM, which is what is used in the model, never becomes larger than one. To clarify, we have introduced a condition statement in Eq. 3 that states that NLIM can not be larger than one. Furthermore, we have included a discussion in Section 2.1.1. (lines 107-111) on that the nutrient limitation is sensitive to the choice of parametrization.

We have also added a discussion around reconstructed limitation patterns compared to the models limitation pattern using N:P ratios and the models inherent definition, NUTLIM, in section 3.2.

The limitation patterns calculated by NUTLIM and N:P ratios clearly show the same trend from P to N limitation over the 20th century but vary quite a bit for different months (Fig. 9). Which of these limitation functions best capture the real world is hard to say, given how variable the Redfield ratio has been found to be in phytoplankton. However, for our model results this is not a problem, as these are undeniably controlled by NUTLIM.

3. *The laconic Section on river loads looks now better. Although, the strong inter-annual coherence (with only 1 year lag?) between local riverine input and DIN in the mixed layer (L255) deserves more consideration and explanation, remembering although about open boundaries with the gulfs and the south-western Baltic. On the other hand, the anti-phase coherence between salinity and DIN on periodicities $\gtrsim 1$ yr, might has the same reason as the in-phase coherence between salinity and phosphate, that is the upward transport of deep waters due to hypoxia enriched with DIP and depleted in DIN. Could be worth mentioning as pertinent to the vicious circle of Baltic Sea eutrophication that is more appropriate here than in the Section on limitation.*

We have added a discussion on this in section 3.3.

4. *The Summary and conclusion Section contains too much repetition or just a prolongation of the awkward discussion from the preceding Results and discussion Section, including even some contradictions with dates and chronology. It must be effectively cut down to just the conclusions.*

We agree and have significantly shortened section 4. focusing on just the conclusions.

Minor suggestions

We have revised the manuscript in accordance with the minor suggestions.

Response to Referee #3

We thank the referee for valuable comments on the manuscript.

The concern about lack of comparison with observations were put forward by both referees. We have added references to studies which includes validation of the particular run used in our manuscript. We have further included a validation of simulated phytoplankton at monitoring station BY15.

The minor comments have been addressed.

Causes of simulated long-term changes in phytoplankton biomass in the Baltic Proper: A wavelet analysis

Jenny Hieronymus¹, Kari Eilola¹, Magnus Hieronymus¹, H. E. Markus Meier^{2,1}, Sofia Saraiva¹, and Bengt Karlsson¹

¹Research and Development Department, Swedish Meteorological and Hydrological Institute, Norrköping, Sweden

²Department of Physical Oceanography and Instrumentation, Leibniz Institute for Baltic Sea Research Warnemünde, Rostock, Germany.

Correspondence to: Jenny Hieronymus (jenny.hieronymus@gmail.com)

1 **Abstract.** The co-variation of key variables with simulated phytoplankton biomass in the Baltic proper has been examined using wavelet analysis and results of a long-term simulation for 1850-2008 with a high-resolution, coupled physical-biogeochemical circulation model for the Baltic Sea. By focusing on inter-annual variations it is possible to track effects acting on decadal time scales such as temperature increase due to climate change as well as changes in nutrient input. The **results** indicate the largest strongest inter-annual coherence of phytoplankton biomass with indicates that variations in phytoplankton biomass are determined by changes in concentrations of the limiting nutrient. However, after 1950 the coherence is reduced due to high mixed layer nutrient concentrations diminishing the effect of smaller long-term variations high nutrient concentrations created a less nutrient limited regime and the coherence was reduced. Furthermore, the inter-annual coherence of mixed layer nitrate with riverine input of nitrate is much larger than the coherence between mixed layer phosphate and phosphate loads. This indicates a greater relative importance of mixing the vertical flux of phosphate from deeper layers the deep layer into the mixed layer. In addition, shifts in nutrient patterns give rise to changes in phytoplankton nutrient limitation. The modelled pattern shifts from purely phosphate limited to a seasonally varying regime. The results further indicate some effect of inter-annual temperature increase on cyanobacteria and flagellates. Changes in mixed layer depth affect mainly diatoms due to a high sinking velocity while inter-annual coherence between irradiance and phytoplankton is not found.

15 1 Introduction

16 The Baltic Sea is a semi-enclosed brackish water body separated from the North Sea and Kattegat through the Danish Straits. It stretches from about 54° to 66° N and the limited water exchange with the ocean in the south gives rise to a large meridional salinity gradient. The circulation is estuarine with a salty deep-water inflow from the ocean and a fresher surface outflow. The Baltic Sea comprises a number of sub-basins connected by sills further restricting the circulation.

20 The limited water exchange and the long residence time of water have consequences for the biology and the biogeochemistry. The Baltic Sea is naturally prone to eutrophication and organic matter degradation keeps the leads to low deep water oxygen concentrations generally low in between deep water renewal events. In turn, this leads to complex nutrient cycling with different processes acting in oxygenized vs low oxygen environments.

24 The Baltic Sea has experienced extensive anthropogenic pressure over the last century. After 1950, intensive use of agricultural fertilizer greatly enhanced the nutrient loads. This led to an expansion of hypoxic bottoms (Carstensen et al., 2014), in turn affecting the cycling of nutrients through the system. Anoxic sediments have lower phosphorus retention capacity resulting in increased deep water phosphate concentrations. Thereby, the flux of phosphate to the surface ~~intensifies intensified~~ even though the external loads ~~have~~ decreased after 1980 in response to improved sewage treatment. Furthermore, as the anoxic area ~~increases increased~~, the area of interface between oxic and anoxic zones where denitrification occurs also ~~increases. This results increased. This resulted~~ in a loss of nitrogen. Vahtera et al. (2007) described these processes as generating a “vicious circle” where decreased DIN concentrations together with increased phosphate ~~enhance enhanced~~ the relative importance of nitrogen fixation by cyanobacteria.

33 The importance of this coupling between oxygen and nutrients have been ~~further~~ examined in models. Gustafsson et al. 34 (2012) confirmed, using the model BALTSEM, that internal nutrient recycling has increased due to ~~the~~ reduced phosphate 35 retention capacity, ~~implicating resulting in~~ a self sustained eutrophication where enhanced ~~internal loads sedimentary outflux~~ 36 ~~of nutrients together with increased nitrogen fixation~~ outweigh external load reductions.

37 Satellite monitoring has made it possible to observe changes in several physical and ecological surface variables during the 38 past three decades. Significant changes in seasonality have been observed, such as ~~an~~ earlier start of ~~the~~ phytoplankton growth 39 season and timing of chlorophyll maxima (Kahru et al., 2016).

40 ~~Although the satellite record is already substantial and growing, interannual shifts and variations over the past century can 41 not be investigated in this way. Furthermore, the satellite record is restricted to a few surface variables.~~

42 Shifts in nutrient composition and deep water ~~variables properties~~ remain difficult to evaluate using observations. Even 43 though the Baltic Sea has a dense observational record from ships, stations and satellites, the longest nutrient records comprise 44 station data from the early ~~70s-1970~~ (HELCOM, 2012). For ~~multideadal periods of gap free data longer time periods~~ the use 45 of a model is required.

46 In this paper we construct a thorough analysis of the co-variation of phytoplankton biomass with key variables that have 47 been affected by anthropogenic change over the 20th century. Using the biogeochemical model SCobi (Eilola et al., 2009; 48 Almroth-Rosell et al., 2011) coupled to the 3d circulation model RCO ([Meier et al., 2003](#)) we scrutinize the effect of nutrient 49 loads, nutrient concentration, temperature, irradiance and mixed layer depth on the modelled phytoplankton community.

50 The gap-free dataset provided by the model ~~lets us allows us to~~ decompose the variables in time-frequency space using the 51 wavelet transform. Two variables may than be compared using wavelet coherence ([eg. Torrence and Compo, 1998; Grinsted et al., 2004](#)) ([e](#))

52 We have chosen to use a model run spanning ~~1850-2009~~ ~~the period 1850 to 2009~~. Thereby, we capture conditions relatively 53 unaffected by anthropogenic forcing as well as current conditions of eutrophication and climate change. Furthermore, we limit 54 our investigation to the Baltic Proper so as to capture relatively homogenous conditions with regards to the biology.

55 ~~Schimanke and Meier (2016) analyzed multideadal variations in Baltic Sea salinity and the coherence with different physical 56 drivers. They used the wavelet transform to identify periodicities and wavelet coherency to analyse the driving mechanisms.~~

57 **2 Methods**

58 **2.1 Study area**

59 The Baltic Sea contains several different sub-basins with different characteristics in salinity and nutrient loads. We have here
60 chosen to focus on the Baltic Proper. To obtain homogenous conditions we focus on the open ocean away from coasts. Areas
61 where the depth is less than 20m are therefore removed. The study area is displayed in Fig. 1.

62 We have chosen to use a basin averaged approach. All variables have thus been horizontally averaged over the study area.
63 This way we remove local variability and hope to gain a better understanding of the system.

64 **2.1 Model**

65 We have used a run with from the model RCO-SCOBI spanning 1850-2009. RCO (Rossby Centre Ocean model) is a three-
66 dimensional regional ocean circulation model (Meier et al., 2003). It is a z-coordinate model with a free surface and an open
67 boundary in the northern Kattegat. The version used here has a horizontal resolution of 2nm with 83 depth levels at 3m intervals.

68 The biogeochemical interactions are solved by the Swedish Coastal and Ocean Biogeochemical model (SCOBI) (Eilola
69 et al., 2009; Almroth-Rosell et al., 2011). The model solves for three different water column and benthic nutrients (contains the
70 nutrients phosphate, nitrate and ammonia) as well as the plankton functional types representing diatoms, flagellates and others
71 (will be referred to as flagellates from here on) and cyanobacteria. Furthermore, the model contains nitrogen and phosphorus
72 in one active homogenous benthic layer.

73 The model equations can be found in Eilola et al. (2009). Since we are exploring the effect of different variables on the
74 growth of phytoplankton we will, for clarity, repeat some of them here.

75 The phytoplankton biomass is described in terms of chlorophyll and with a constant C:Chl ratio. The model thus does not
76 take into account seasonal changes in C:Chl as was found by Jakobsen and Markager (2016).

77 The net growth of phytoplankton (PHY) is described by the following expression,

$$78 \text{GROWTH}_{\text{PHY}} = \text{ANOX} \cdot \text{LTLLIM} \cdot \text{NUTLLIM}_{\text{PHY}} \cdot \text{GMAX}_{\text{PHY}} \cdot \text{PHY}, \quad (1)$$

79 where subscript PHY indicates the plankton functional type (diatoms, flagellates or cyanobacteria). ANOX is a
80 logarithmic expression that approaches zero as the oxygen concentration becomes small.

81 LTLLIM expresses the phytoplankton light limitation and NUTLLIM describes the nutrient limitation. Nutrient limitation
82 follows Michaelis-Menten kinetics where constant Redfield ratios are assumed in nutrient uptake. NUTLLIM is further described
83 in Sects. 2.1.1 and 2.1.2. GMAX is temperature dependent and describes the maximum phytoplankton growth rate.

84 The difference between diatoms and flagellates are present in Diatoms and flagellates have different halfsaturation con-
85 stants, maximum growth rate, temperature dependence and sinking rate. Flagellates are more sensitive to a change changes in
86 temperature than diatoms. Furthermore, the sinking rate of diatoms is five times larger than that for flagellates.

87 The difference between cyanobacteria and the other phytoplankton ~~species~~ is more pronounced. Cyanobacteria can grow ei-
88 ther according to Eq. (1) or using nitrogen fixation. The rate of nitrogen fixation ~~as is~~ a function of ~~the phosphate concentration phosphate~~
89 ~~concentration, N:P ratio~~ and temperature. Both ~~N₂-fixation~~ nitrogen fixation and GROWTH of cyanobacteria is zero if the salinity
90 is above 10. Furthermore, cyanobacteria is the most temperature sensitive of the phytoplankton groups and no sinking ~~velocity~~
91 is assumed.

92 Other processes important for our results involves chemical reactions occurring in the water column or in the sediment.
93 Denitrification occurs ~~in both~~ both in the water column and the benthic layer and constitutes a sink for nitrate in case of anoxia.
94 Nitrification transforms ammonium into nitrate as long as oxygen is present. Phosphorus is adsorbed to the sediment and the
95 benthic release capacity of phosphate is a function of the oxygen concentration ~~where more oxygen implies less release~~. The
96 phosphorus release capacity is also dependent on salinity ~~where higher salinity means less phosphate is retained whereby~~
97 ~~higher salinity leads to lower retention of phosphate~~ in the benthic layer.

98 2.1.1 Nutrient limitation

99 Estimating nutrient limitation in nature is difficult. Usually this is done, either by comparing nutrient ratios to Redfield ~~in e.g.~~
100 ~~e.g.~~ the surface water or external supply or ~~by some nutrient enrichment experiment through nutrient enrichment experiments~~
101 (Granéli et al., 1990).

102 The ~~idea implementation~~ of nutrient limitation ~~as often used is based on most commonly used is~~ that the primary production
103 is directly limited by the nutrient concentration in the ambient water and that the internal nutrient ratios in the phytoplankton are
104 constant, i.e. ~~in~~ accordance with a Redfield-Monod model (Redfield, 1958). However, cell-quota type models (Droop, 1973)
105 are being increasingly implemented and the use of constant internal nutrient ratios are becoming more and more questioned
106 (~~Flynn, 2010~~) (~~Flynn, 2010; Fransner et al., 2018~~).

107 ~~Furthermore, N vs P limitation is a long-standing debate. Tyrrell (1999) uses a box-modelling approach to show that in~~
108 ~~steady state, nitrogen becomes slightly deficient while it is the external input and removal of phosphate that ultimately controls~~
109 ~~the production.~~

110 Here, ~~In our model~~, nutrient limitation is ~~traditionally expressed assuming constant~~ expressed assuming constant Redfield
111 ratios and phytoplankton growth is limited by either nitrogen or phosphate. The degree of nutrient limitation is described by ~~as~~

$$112 \text{NUTLIM}_{\text{PHY}} = \min(\text{NLIM}_{\text{PHY}}, \text{PLIM}_{\text{PHY}}) \quad (2)$$

113 where NLIM_{PHY} and PLIM_{PHY} are the nitrogen and phosphate limitation respectively. ~~In addition, NLIM_{PHY} contains the~~
114 ~~sum of the nitrate and ammonium limitation, i.e. is defined as~~

$$115 \text{NLIM}_{\text{PHY}} = \begin{cases} \text{NO}_3\text{LIM}_{\text{PHY}} + \text{NH}_4\text{LIM}_{\text{PHY}}, & \text{if } \text{NO}_3\text{LIM}_{\text{PHY}} + \text{NH}_4\text{LIM}_{\text{PHY}} \leq 1 \\ 1, & \text{otherwise,} \end{cases} \quad (3)$$

116 where

117 $\text{NO}_3\text{LIM} = \frac{\text{NO}_3}{\text{KNO}_3\text{PHY} + \text{NO}_3} \cdot \exp(-\phi_{\text{PHY}} \cdot \text{NH}_4),$ (4)

118 $\text{NH}_4\text{LIM} = \frac{\text{NH}_4}{\text{KNH}_4\text{PHY} + \text{NH}_4},$ (5)

119 where NO_3 and NH_4 are the concentrations of nitrate and ammonium and KNO_3PHY and KNH_4PHY are the halfsaturation constants for nitrate and ammonium respectively. The exponent in (4) accounts for inhibition of nitrate uptake (e.g. Dortch (1990); Parker (1993)) (e.g., Dortch, 1990; Parker, 1993).

122 PLIM_{PHY} is modelled as, equal to PO_4LIM which is modelled as

123 $\text{PO}_4\text{LIM} = \frac{\text{PO}_4}{\text{KPO}_4\text{PHY} + \text{PO}_4}.$ (6)

124 Nutrient limitation, NUTLIM, is thus described by a number between 0 and 1 where 1 is no limitation. Note that NLIM The
 125 constant KPO_4PHY is the half saturation constants for phosphate and the constant ϕ_{PHY} in Eq. (3) may obtain values larger
 126 than 1. However, as 4) determines the strength of ammonium inhibition of nitrate uptake. Since NUTLIM is calculated as the
 127 minimum of NLIM and PLIM, NLIM larger than one will always mean P limitation. PLIM will temporally cause P limitation
 128 of phytoplankton growth rate. Hence, a different formulation e.g. of NLIM might change a models sensitivity to the limiting
 129 nutrient. Its impact on system nutrient dynamics on longer time scales is, however, difficult to judge because e.g. nitrogen
 130 fixation and denitrification potentially also may be influenced. Further experiments on this issue are out of the scope of the
 131 present paper and left for future studies.

132 The constants KNO_3PHY , KNH_4PHY and KPO_4PHY are the half saturation constants and differs between the different
 133 phytoplankton groups. The constant ϕ_{PHY} in NUTLIM for our model run has been calculated offline from the monthly means
 134 according to Eq. (4) determines the strength of ammonium inhibition of nitrate uptake 2).

135 2.1.2 Effect of physical parameters

136 Changes in cloud-cover affect the incoming solar radiation and thereby the phytoplankton growth. The effect of light shows up
 137 in is given by the LTLIM term of Eq. (1) which accounts for photo-inhibition.

138 The mixed layer depth has been defined as the depth where a density difference of 0.125 kg m^{-3} from the surface is reached
 139 occurs in accordance with what was previously done by e.g., Eilola et al. (2013). The density was calculated from modelled
 140 temperature and salinity using the algorithms from Jackett et al. (2006).

141 2.2 Study area

142 The Baltic Sea contains several different sub-basins with different characteristics in salinity and nutrient loads. In this study
 143 we focus on the Baltic proper as defined in Fig. 1. In order to reduce heterogeneity we exclude areas shallower than 20m and
 144 put our focus away from the coasts.

145 We have chosen to use a basin averaged approach in order to remove local variability and gain a better understanding of
146 the system. All variables have thus been horizontally averaged over the study area. Furthermore, we have also averaged all
147 variables over the mixed layer and from the mixed layer down to a depth of 150m.

148 2.3 Forcing

149 The study use reconstructed (1850-2008) atmospheric, hydrological and nutrient load forcing and daily sea levels at the lateral
150 boundary as described by Gustafsson et al. (2012) and Meier et al. (2012). Monthly mean river flows were merged from
151 reconstructions ~~done~~ by Hansson et al. (2011) and ~~by~~ Meier and Kauker (2003) and hydrological model data ~~by~~ ~~from~~ Graham
152 (1999), respectively. For further details about the physical model setup used in the present study the reader is referred to
153 [Meier et al. \(2016\)](#) and references therein.

154 The nutrient ~~loads~~ input from rivers and point sources were (1970-2006) compiled from the Baltic Environmental and HEL-
155 COM databases (Savchuk et al., 2012). Estimates of pre-industrial loads for 1900 were based ~~upon~~ on data from Savchuk et al.
156 (2008). The nutrient loads were linearly interpolated between selected reference years in the period between 1900 and 1970.
157 Similarly, atmospheric loads were estimated (Ruoho-Airola et al., 2012). Nutrient loads contain both organic and inorganic
158 phosphorus and nitrogen, respectively. For riverine organic phosphorus and nitrogen loads bioavailable fractions of 100 and
159 30% are assumed, respectively.

160 [Figure](#) The upper panel of Fig. 2 shows the ~~loads~~ input of Dissolved Inorganic Phosphorus (DIP, ~~top~~) and Dissolved Inorganic
161 Nitrogen (DIN, ~~bottom~~) to the Baltic Proper as defined in Fig. 1. The ~~loads~~ are shown together with lower panel shows the
162 corresponding simulated mixed layer ~~e~~ concentration concentrations. The loads ~~are~~ have been calculated from the runoff and
163 annual mean nutrient concentrations (Eilola et al., 2011). Thus the seasonal cycle in river loads is determined by the runoff.
164 After a spin-up simulation for 1850-1902 utilizing the reconstructed forcing as described above, the calculated physical and
165 biogeochemical variables at the end of the spin-up simulation were used as initial condition for 1850. We have used riverine
166 DIN and DIP loads for our analysis. The use of total bioavailable nutrient loads instead does not change the results.

167 The open boundary conditions in the northern Kattegat were based on climatological (1980-2000) seasonal mean nutrient
168 concentrations (Eilola et al., 2009). Similar to Gustafsson et al. (2012) a linear decrease of nutrient concentrations back in
169 time was added assuming that climatological concentrations in 1900 amounted to 85% of present day concentrations (Savchuk
170 et al., 2008). The bioavailable fraction of organic phosphorus at the boundary was assumed to be 100% in accordance with
171 the organic phosphorus supply from land runoff. Organic nitrogen was implicitly added because of the Redfield ratio of model
172 detritus (Eilola et al., 2009).

173 2.4 Evaluation

174 The specific model setup used here have been shown to agree well with observations for salinity, temperature and nutrients
175 (Meier et al., in press; Eilola et al., 2014). The different phytoplankton functional types have not been previously validated
176 against observations.

177 Fig. 3 shows the different simulated phytoplankton together with observations at the monitoring station BY15 (see Fig.1).
178 Monthly means and standard deviations are shown in Fig. 4. The observational dataset has been recalculated from biovolumes
179 to carbon units in accordance with Menden-Deuer and Lessard (2000). The simulated values have been recalculated from units
180 of chlorophyll to carbon through a fixed C:Chl ratio of 50 which is in the mid range of the salinity dependent span found by
181 Rakko and Seppälä (2014).

182 The time-series display significant interannual variability in both model and observations. This variability is also visible
183 as large standard deviations in the modelled and observed monthly means in Fig. 4. Fig. 4 also shows an autumn diatom
184 bloom in the observations while the model generates an autumn flagellate bloom. The simulated cyanobacteria bloom occurs
185 approximately two months too late compared to observations. It is also notable that the cyanobacteria displays strong blooms
186 the first four years in both model and observations but that the observations show diminished blooms during the rest of the
187 period where the simulated biomass is still high.

188 Differences in absolute numbers between observations and simulated values can result from the choice of the fixed Chl:C
189 ratio. Furthermore, the estimated carbon content from observations are potentially affected by patchiness during in-situ sampling
190 and uncertainties related to the calculation of biovolumes and transformation to carbon units.

191 2.5 The wavelet transform and wavelet coherence

192 Several ~~referencees explain~~ studies have covered the wavelet transform and its application in depth (e.g. Lau and Weng (1995),
193 Torrence and Compo (1998), Carey et al. (2016), Grinsted et al. (2004)) and we will here provide a brief introduction (e.g., Lau and Weng
194 here we provide a description of the method.

195 The continuous wavelet transform provides a method to decompose a signal into time-frequency space. In that it is similar
196 to the windowed Fourier transform where the signal is decomposed within a fixed time-frequency window which is then slided
197 along the time-series. However, the fixed width of the window leads to an underestimation of low frequencies. In comparison,
198 the wavelet transform utilizes wavelets with a variable time-frequency window. Wavelets can have many different shapes and
199 the choice is not arbitrary. We have chosen the commonly used Morlet wavelet providing good time and frequency localization
200 (Grinsted et al., 2004).

201 In time-series with clear periodic patterns ~~that is~~ affected by environmental variables such as population dynamics and
202 ecology the benefits with of this approach are significant (Cazelles et al., 2008). In recent years, several ~~referencees~~ studies
203 have highlighted the usefulness of wavelet analyses in plankton research (Winder and Cloern, 2010; Carey et al., 2016). The
204 focus ~~have has~~ been the increased availability of long observational data sets making it possible to use the wavelet transform
205 ~~for investigation of to investigate~~ changes in seasonality. Carey et al. (2016) discussed how the wavelet transform can be
206 used to track interannual changes in phytoplankton biomass and applied it to a 16-year time series of phytoplankton in Lake
207 Mendota, USA. In doing ~~this so~~ they were able to identify periods when the annual periodicity was less pronounced. They
208 ~~discuss discussed~~ the benefit of this technique in scrutinizing changes to the seasonal succession due to changes in external
209 drivers. Winder and Cloern (2010) applied the technique to time-series of chlorophyll-a from marine and freshwater localities
210 and discussed the annual and seasonal periodicities.

211 Wavelet coherence further expands the usefulness of the wavelet approach by allowing ~~for calculating calculation~~ of the time
212 resolved coherence between two time-series (Grinsted et al., 2004; Cazelles et al., 2008). In this way, it is possible to identify
213 transient periods of correlation over different periodicities. The result is given as coherency as a function of time and period as
214 well as a phase lag between the two time-series.

215 The problem with the wavelet transform is that it requires a dataset without gaps. The time-series also needs to be sufficiently
216 long~~compared to the investigated periods. This makes it difficult to use the method to scrutinize the coherence of processes~~
217 ~~acting on longer time-scales, such as climate change, since long enough. This impedes the wavelet analysis on longer time~~
218 ~~scales such as the time scale of changing climate because long~~ observational datasets are ~~scarce~~lacking. Hence, for our purpose
219 only a model based approach is feasible.

220 Schimanke and Meier (2016) used wavelet coherency on a multi-centennial model run to evaluate the correlation of different
221 forcing variables with the Baltic Sea salinity. ~~We will here scrutinize~~ ~~Here we analyze~~ the coherence between modelled
222 phytoplankton biomass and a few key modelled and forcing variables.

223 For all wavelet calculations we use the Matlab wavelet package ~~of~~ described in Grinsted et al. (2004), which is freely
224 available at <http://www.glaciology.net/wavelet-coherence>.

225 3 Results and discussion

226 ~~The results shown are monthly means averaged over the basin. The different variables have also been vertically averaged over~~
227 ~~the mixed layer and/or from the mixed layer down to a depth of 150m.~~

228 We will begin in Sect. 3.1 by presenting the model results ~~of phytoplanton~~ ~~on phytoplankton~~ biomass. In Section 3.2 we will
229 ~~consider the composition of nutrients and the~~ ~~present the nutrients and their~~ coherence with the phytoplankton biomass. Co-
230 herence between riverine loads and mixed layer nutrients will be discussed in Sect. 3.3. Section 3.4 examines the coherence of
231 phytoplankton with temperature and irradiance. Finally, the coherence between mixed layer depth and phytoplankton biomass
232 is considered in Sect. 3.5. ~~All results shown are monthly means.~~

233 3.1 Phytoplankton biomass

234 Fig. 5 shows the time-series of phytoplankton biomass (a) together with the corresponding wavelet spectrum (b).

235 The wavelet power (variance) of the decomposed signal (in color) is displayed as a function of time (x-axis) and period
236 (y-axis). The black curves in Fig. 5(b) show the 95% confidence level relative to red noise.

237 Averaging over time generates the global power spectrum displayed in Fig. 5 (c). The wavelet spectrum clearly reveals two
238 main periodicities - the annual and the semi-annual representing the spring and autumn blooms. It is also clearly visible that
239 the power on both periodicities increases markedly after 1950.

240 Kahru et al. (2016) found a shift in chlorophyll maxima from the diatom dominated spring bloom to the cyanobacteria
241 summer bloom. ~~Fig. 6 shows that a~~ ~~A~~ similar pattern emerges from our model run ~~with five years of cyanobacterial chlorophyll~~
242 ~~maxima occurring after 1998~~ ~~as can be seen in Fig. 6. The figure shows the month of maximum biomass of the different~~

243 phytoplankton species as well as the month of maximum chlorophyll (diatoms+flagellates+cyanobacteria). After 1998 the
244 results display five years where the month of maximum chlorophyll corresponds to the month of maximum cyanobacteria
245 biomass in August or September.

246 3.2 Nutrients and nutrient limitation

247 ~~The extent of anoxic bottoms in the Baltic Sea has increased markedly over the past century. Carstensen et al. (2014) found~~
248 ~~Increased nutrient loads have caused a strengthening of the primary production and thereby also the deep water respiration,~~
249 ~~resulting in a 10-fold increase in the hypoxic area since the beginning of the 20th century. They explained this to be primarily~~
250 ~~due to increased nutrient loads causing increased primary production and resulting in an enhanced deep water respiration.~~

251 ~~Changing nutrient patterns in the Baltic Sea due to spreading hypoxia (Carstensen et al., 2014) . This has lead to changing~~
252 ~~nutrient patterns as~~ have been discussed by e. g. Conley et al. (2002); Savchuk (2010); Vahtera et al. (2007) . (e.g., Conley et al., 2002; Sav-

253 Anoxia causes sedimentary phosphate release. A clear relationship between hypoxia and total basin averaged phosphate was
254 first shown by Conley et al. (2002) (and later expanded by Savchuk (2010)) on observational data from the Baltic Proper.

255 The effect of hypoxia on DIN is less straight forward. Expanding hypoxia increases the boundary area between anoxic and
256 oxic water where denitrification occurs resulting in a ~~further~~ loss of nitrate. Furthermore, hypoxia ~~induced causes a~~ reduction
257 in nitrification ~~results in a loss of leading to a further reduction in~~ nitrate. Vahtera et al. (2007) found a negative relationship
258 between basin averaged DIN and hypoxic area in observations from the Baltic ~~sea~~Sea.

259 ~~We illustrate the~~ The changing nutrient patterns for our model run ~~are shown~~ in Fig. 7. In conjunction with the increased
260 anoxic volume we find a clear increase in ammonium and a decrease in nitrate. This is due to a decrease in nitrification and an
261 increase in denitrification. The phosphate concentration increases from the mid 20th century through the rest of the model run
262 as a combined effect of the accumulated terrestrial inputs and hypoxic sedimentary release.

263 The effect of nutrients on the primary production is in the model controlled by the term NUTLIM, or degree of nutrient
264 limitation, in Eq. (1). NUTLIM can be viewed as a measure of the nutrient composition that linearly affects the phytoplankton
265 growth in the model. We ~~will~~ examine this term in ~~and as well as~~ below the mixed layer ~~. Even though there is no primary~~
266 ~~production in the deep water and thus the nutrient limitation term has no effect here, a shift in the composition as changes in the~~
267 ~~concentration~~ of nutrients in the deep water will affect also ~~nutrient concentrations in~~ the mixed layer. ~~NUTLIM for diatoms~~
268 ~~and flagellates has been calculated offline from the monthly means according to Eq. (2).~~

269 The evolution

270 ~~The evolutions~~ of NUTLIM in the ~~surface layer and the mixed layer and~~ deep water for diatoms and flagellates ~~is are~~ shown
271 in Fig. 8. There is a clear increase over the 20th century and a shift towards less limited conditions (NUTLIM approaching 1).

272 Nitrogen has been shown to most often ~~be limiting limit the growth~~ in the Baltic Proper, while phosphate is limiting in
273 the northern basins (Granéli et al., 1990; Tamminen and Andersen, 2007). Schernewski and Neumann (2004) showed through
274 ~~a reconstruction of the Baltic Sea trophic state in the early 1900 that~~ In pre-industrial conditions, N/P ratios indicate a lesser
275 ~~degree of nitrogen limitation and a higher degree of phosphate limitation for the central Baltic Sea (Schernewski and Neumann, 2004; Savchuk,~~
276 ~~The mixed layer limitation pattern in our model run as calculated with~~ N/P ratios ~~in the Baltic Proper have decreased but that~~

277 much of the domain still indicated N limitation is shown in the lower panel of Fig. 9. Until 1980 the results show a pattern
278 of limitation shifting between nitrogen and phosphate whereafter persistant N limitation develops. This weaker N limitation
279 during the first part of the run is consistant with above mentioned studies of pre-industrial conditions.

280 Using the models definition of nutrient limitation, our model results, shown in Fig. 9, display phosphate limitation for both
281 diatoms and flagellates for the earlier part of the run. After 1980, seasonality appears in the mixed layer. Phosphate is a different
282 seasonal pattern appears with phosphate still limiting during winter while nitrogen becomes limiting after the spring bloom.
283 Calculating Even though the limitation pattern as calculated with NUTLIM differs from what was found using N/P ratios as
284 a more conventional measure of nutrient limitation, our model results display instead a shifting pattern until 1976 whereafter
285 persistant N limitation develops (not shown), the overall pattern of increasing degree of N limitation is evident in NUTLIM as
286 well.

287 The changing nutrient patterns affects the limitation patterns affect phytoplankton growth. We analyse the wavelet coheren-
288 cies of phytoplankton biomass with mixed layer phosphate and DIN in Figs. 10 and 11.

289 Coherency is shown in color as a function of year (x-axis) and period (y-axis). More yellow indicates stronger coherence. The
290 arrows reveal the phase-lag between the two time-series. The line plots on the right show the time-averaged coherence. As the
291 strongest nutrient limited group, diatoms show persistant inter-annual coherence with phosphate during the first, consistently
292 phosphate limited part of the run (see Fig. 10, see also Fig. 9). During the later part of the run the nutrient and phytoplankton
293 concentrations are high enough that smaller inter-annual variations have little effect.

294 Since nitrogen limitation in the model only as calculated with NUTLIM mostly occurs after 1980 and after the spring
295 bloom (Fig. 9), and thus only affects the much smaller diatom and flagellate autumn blooms no little coherence between
296 phytoplankton and nitrogen is visible in can be observed on inter-annual time-scales (Fig. 11).

297 To scrutinize the shift in deep water nutrient composition and the coherence with phytoplankton, we calculate the wavelet
298 coherence between below mixed layer NUTLIM and the diatom and flagellate biomass. The result is shown in Fig. 12. The
299 phase arrows here display some interesting features. After 1980 the phase arrows within the annual coherence period change to
300 the opposite direction. For diatoms, the phase shifts from NUTLIM preceding diatoms by three months to diatoms preceding
301 nutlim NUTLIM by the same amount. Flagellates display a similar shift.

302 To investigate this, we have plotted the The month of maximum NUTLIM shown in Fig. 13. The figures show, indicates
303 the month when the nutrient composition is most beneficial for phytoplankton growth. The figure shows a clear shift occurring
304 after 1980. Below the mixed layer, NUTLIM changes its maxima from December and January to July, August and September
305 for both diatoms and flagellates while a slight shift from February to March is apparent occurs in mixed layer NUTLIM for
306 diatoms. Mixed layer NUTLIM for flagellates displays no clear shift. The shift in NUTLIM is a result of the increase in
307 phosphate and ammonium occurring in conjunction with the increase in anoxic volume shown in Fig. 7. The change in timing
308 is probably due to reduced sedimentary phosphate retention and reduced nitrification after the spring bloom.

309 3.3 Nutrient loads

310 We here analyze how changes in nutrient loads affect changes in the mixed layer nutrient concentrations.

311 The wavelet coherence between mixed layer nutrients and riverine input is shown in Fig. 14. ~~We have used riverine DIN and~~
312 ~~DIP loads in the results presented below. The use of instead total bioavailable nutrient loads does not change the results.~~

313 The phosphate loads show little coherence on periodicities longer than one year but DIN displays strong inter-annual co-
314 herence. The phase-arrows indicate a phase-lag of about minus 45° on all inter-annual periodicities. For an 8 year period this
315 means that a change in riverine input precedes changes in mixed layer DIN by about 1 yr.

316 To further investigate the lack of inter-annual coherence between riverine phosphate loads and mixed layer phosphate, the
317 wavelet coherence between mixed layer salinity and nutrients are examined and displayed in Fig. 15. Mixed layer salinity is
318 affected by freshwater input from land, water exchange with adjacent basins, precipitation, evaporation and mixing with deeper
319 layers. The coherence spectrum reveals higher coherence between mixed layer salinity and phosphate (top) on interannual
320 periodicities than between salinity and DIN (bottom). The coherence ~~existing that does exist~~ between salinity and DIN on
321 periodicities longer than one year is antiphase i.e. low salinity here coheres with high DIN concentrations. This indicates that
322 high runoff is connected to high nitrogen loads and high DIN concentrations in the mixed layer. It is also possible that low
323 salinity in the mixed layer indicate periods with deep mixing and better oxygen conditions in and below the halocline (?) . This
324 could reduce the denitrification during these periods and thus result in higher mixed layer DIN concentrations.

325 In contrast, the stronger inter-annual in-phase coherence between salinity and phosphate suggests that the reason for the
326 coherence might be a greater importance of phosphorus release from the sediments that eventually reaches the mixed layer
327 through mixing with deeper layers (cf. Eilola et al., 2014).

328 Riverine nutrient loads show little inter-annual coherence with phytoplankton biomass (not shown) other than on a 16 yr
329 period which probably reflects the overall pattern of simultaneous increase in riverine loads and phytoplankton biomass over
330 the second half of the 20th century.

331 3.4 Temperature and irradiance

332 The mixed layer temperature has increased over the 20th century. ~~Figure ?? shows the 2-yr moving average of mixed~~
333 ~~layer temperature. To scrutinize (not shown). To analyze~~ the effect of temperature on the ~~concentration of phytoplankton~~
334 ~~phytoplankton biomass~~, the wavelet coherence between temperature and phytoplankton have been plotted in Fig. 16. The re-
335 sults suggest that the temperature increase after 1990 might have had an effect on cyanobacteria and flagellates. It is also
336 noticeable that the temperature increase observed between 1900 and 1940 probably had an effect on cyanobacteria. This is also
337 in agreement with the model formulation where cyanobacteria are the most sensitive to temperature followed by flagellates.

338 Light impacts primary production through the term LTLIM in Eq. (1). However, irradiance display very little variation on
339 any other periodicity than the annual as can be observed in a wavelet power spectrum (not shown). Therefore there exists
340 almost no coherence between phytoplankton and irradiance apart from the annual and semiannual seasonal signal.

341 3.5 Mixed layer depth

342 ~~The lower panel of Fig. ?? shows the two-year moving average of mixed layer depth averaged over the basin.~~

343 We calculate the coherence between mixed layer depth and diatoms, flagellates and cyanobacteria in Fig. 17.

344 Apart from the annual cycle there is a strong coherence between mixed layer depth and diatoms, and to some extent flagel-
345 lates, on shorter periodicities as well. That is, the ~~concentration of diatoms~~ diatom biomass residing in the mixed layer seems
346 to covary quite well on periodicities equal to or shorter than one year. The model value for diatom sinking rate is five times
347 higher than that for flagellates while cyanobacteria is assumed to have no sinking rate. In a shallow mixed layer the diatom
348 ~~concentration~~ biomass decreases faster than in a deep mixed layer because of the large sinking rate. Furthermore, in a deeper
349 mixed layer stronger turbulence counteract the sinking. In the wavelet coherence spectrum we thus see in-phase short term
350 coherence.

351 4 Conclusions

352 With a focus on simulated inter-annual variations, the wavelet coherence of the mixed layer phytoplankton biomass with key
353 variables affecting the primary production has been examined for the Baltic Proper.

354 ~~We found that the pattern of nutrient limitation in and below the mixed layer have changed in the model since 1980. Below~~
355 ~~the mixed layer, the limitation pattern changes from phosphate to nitrogen for diatoms and to seasonally shifting between~~
356 ~~phosphate and nitrogen. Within the mixed layer, the pattern changes from pure phosphate limitation to seasonally shifting for~~
357 ~~both diatoms and flagellates. This is due to decreased deep water oxygen concentrations and a rapid expansion of anoxia after~~
358 ~~1970. The phosphate concentrations increase due to enhanced sedimentary release, denitrification results in loss of nitrate and~~
359 ~~reduced nitrification decreases the transformation of ammonium to nitrate. The combined effect results in nitrogen limitation~~
360 ~~after the spring bloom which benefits cyanobacteria~~ The simulated chlorophyll concentration maximum shifted from spring to
361 late summer at the end of the 20th century in agreement with Kahru et al. (2016).

362 The ~~mixed layer concentrations of nutrients affect the primary production in the model through the nutrient limitation term,~~
363 ~~NUTLIM. The~~ phytoplankton group most strongly limited by nutrients in the model is diatoms. The connection between
364 primary production and ~~the nutrient limitation term is visable as a~~ nutrients is reflected in the strong inter-annual coherence
365 between diatoms and phosphate as well as NUTLIM before 1940. After 1940 NUTLIM and the ~~concentrations~~ biomass of the
366 individual phytoplankton species have gained such high values that smaller inter-annual variations have relatively little effect
367 on the production. Similarly, ~~the less nutrient sensitive group flagellates shows~~ flagellates which are less limited by nutrients
368 than diatoms show much smaller inter-annual coherence with phosphate even before 1940. NUTLIM for this group is already
369 high enough so high enough that small long-term variations do not reflect strongly in the results.

370 Very little inter-annual coherence is visable observed also between phytoplankton and ~~nitrogen~~. The DIN Using the models
371 definition of nutrient limitation, the spring bloom is phosphate limited throughout the run except for a few years after 1990
372 where diatoms ~~display~~ nitrogen limitation. The much weaker diatom and flagellate autumn bloom displays no inter-annual
373 coherence with DIN most likely due to the high NUTLIM levels.

374 ~~The shift in nutrient limitation patterns is also visable in a slight forward shift in the month of maximum mixed layer~~
375 ~~NUTLIM for diatoms after 1980, although a similar shift cannot be seen for flagellates. Below the mixed layer, maximum~~
376 ~~NUTLIM shifts significantly towards late summer for both diatoms and flagellates. Furthermore, the annual maximum of~~

377 total chlorophyll concentration (Diatoms + Flagellates + Cyanobacteria) displayed a few years at the end of the run where
378 the maximum corresponded to the autumn bloom due to the large increase in cyanobacteria. This is in agreement with
379 Kahru et al. (2016) who found from satellite data that the annual chlorophyll maximum has shifted from the spring bloom
380 maximum in May to the cyanobacteria bloom in July are limited by nitrogen. Calculating instead limitation as given by mixed
381 layer N/P ratios generates a pattern in line with previous estimates (Schernewski and Neumann, 2004; Savchuk et al., 2008; Gustafsson et al.
382

383 Riverine input of nutrients is an extremely important variable in the Baltic Sea and the large increase during the 20th century
384 has initiated spreading of anoxic bottoms (Carstensen et al., 2014). We found quite strong coherence between river-
385 ine input of DIN and mixed layer DIN but not a similar relationship between riverine phosphate input and the corresponding
386 mixed layer concentration. As mixed layer salinity displayed in-phase inter-annual coherence with phosphate and only weak
387 anti-phase coherence with DIN we hypothesise that this is due to a greater importance of the flux of phosphate from lower
388 layers.

389 The mixed layer temperature in the Baltic Proper has increased during the 20th century. We found some response of this
390 mainly from the most temperature sensitive phytoplankton group cyanobacteria during periods of large interannual temperature
391 increases. Flagellates, being more temperature sensitive than diatoms, seems to display a coherence with the temperature
392 increase occurring after 1980.

393 Variations in mixed layer depth affects mainly diatoms as these have a high sinking velocity. In-phase coherence between
394 diatoms and mixed layer depth on periodicities shorter than one year indicates that large seasonal changes in the mixed layer
395 depth significantly affects the mixed layer concentrations diatom biomass, while smaller interannual variations are of little
396 consequence.

397 Irradiance displayed very little coherence with phytoplankton. Interannual variations in irradiance are unimportant for phytoplankton
398 biomass.

399 In conclusion, through studying inter-annual wavelet coherence between simulated phytoplankton biomass and key variables
400 we have found that phytoplankton showed strong coherence with the limiting nutrient before 1950. After that nutrients and
401 phytoplankton exists in the water column at such high concentrations that smaller interannual variations have much less effect.
402 Furthermore, the mixed layer concentrations of DIN show strong interannual coherence with riverine DIN input while riverine
403 phosphate displays almost no coherence with the corresponding mixed layer concentration. Instead, in-phase coherence with
404 mixed layer salinity indicates a stronger importance of mixing with lower layers. Temperature displays some inter-annual
405 coherence with the more temperature sensitive flagellates.

406 5 Data availability

407 The model data on which the results in the present study are based on are stored and available from the Swedish Meteorological
408 and Hydrological Institute. Please send your request to ocean.data@smhi.se.

409 *Acknowledgements.* This work was funded by the Swedish Research Council (VR) within the project “Reconstruction and projecting Baltic
410 Sea climate variability 1850-2100” (Grant 2012-2117).

411 Funding was also provided by the Swedish Research Council for Environment, Agricultural Sciences and Spatial Planning (FORMAS)
412 within the project “Cyanobacteria life cycles and nitrogen fixation in historical reconstructions and future climate scenarios (1850-2100) of
413 the Baltic Sea” (grant no. 214-2013-1449). The study contributes also to the BONUS BalticAPP (Wellbeing from the Baltic Sea - applications
414 combining natural science and economics) project which has received funding from BONUS, the joint Baltic Sea research and development
415 programme.

416 This research is also part of the BIO-C3 project and has received funding from BONUS, the joint Baltic Sea research and development
417 programme (Art 185), funded jointly from the European Union’s Seventh Programme for research, technological development and demon-
418 stration and from national funding institutions.

419 We thank two anonymous referees for their insightful comments and suggestions that greatly improved the manuscript.

420 **References**

421 Almroth-Rosell, E., Eilola, K., Meier, H. E. M., and Hall, P. O. J.: Transport of fresh and resuspended particulate organic material in the
422 Baltic Sea - a model study, *Journal of Marine Systems*, doi:doi:10.1016/j.jmarsys.2011.02.005, 2011.

423 Carey, C. C., Hanson, P. C., Lathrop, R. C., and St. Amand, A. L.: Using wavelet analyses to examine variability in phytoplankton seasonal
424 succession and annual periodicity, *Journal of Plankton Research*, 38, 27–40, doi:10.1093/plankt/fbv116, <http://www.plankt.oxfordjournals.org/lookup/doi/10.1093/plankt/fbv116>, 2016.

425 Carstensen, J., Andersen, J. H., Gustafsson, B. G., and Conley, D. J.: Deoxygenation of the Baltic Sea during the last century, *Proceedings of the National Academy of Sciences*, 111, 5628–5633, doi:10.1073/pnas.1323156111, <http://www.pnas.org/cgi/doi/10.1073/pnas.1323156111>, 2014.

426 Cazelles, B., Chavez, M., Berteaux, D., Ménard, F., Vik, J. O., Jenouvier, S., and Stenseth, N. C.: Wavelet analysis of ecological time series, *Oecologia*, 156, 287–304, doi:10.1007/s00442-008-0993-2, 2008.

427 Conley, D. J., Humborg, C., Rahm, L., Savchuk, O. P., and Wulff, F.: Hypoxia in the Baltic Sea and Basin-Scale Changes in Phosphorus
428 Biogeochemistry, *Environ. Sci. Technol.*, 36, 5315–5320, doi:10.1021/es025763w, 2002.

429 Dortch, Q.: The interaction between ammonium and nitrate uptake in phytoplankton, *Marine Ecology Progress Series*, 61, 183–201,
430 doi:10.3354/meps061183, 1990.

431 Droop, M.: Some thoughts on nutrient limitation in algae, *Journal of Phycology*, 9, 264–272, doi:10.1111/j.1529-8817.1973.tb04092.x, 1973.

432 Eilola, K., Meier, H. E. M., and Almroth, E.: On the dynamics of oxygen, phosphorus and cyanobacteria in the Baltic Sea; A model study, *Journal of Marine Systems*, 75, 163–184, doi:10.1016/j.jmarsys.2008.08.009, <http://dx.doi.org/10.1016/j.jmarsys.2008.08.009>, 2009.

433 Eilola, K., Gustafsson, B. G., Kuznetsov, I., Meier, H. E. M., Neumann, T., and Savchuk, O. P.: Evaluation of biogeochemical
434 cycles in an ensemble of three state-of-the-art numerical models of the Baltic Sea, *Journal of Marine Systems*, 88, 267–284,
435 doi:10.1016/j.jmarsys.2011.05.004, <http://dx.doi.org/10.1016/j.jmarsys.2011.05.004>, 2011.

436 Eilola, K., Mårtensson, S., and Meier, H. E. M.: Modeling the impact of reduced sea ice cover in future climate on the Baltic Sea biogeo-
437 chemistry, *Geophysical Research Letters*, 40, 149–154, doi:10.1029/2012GL054375, 2013.

438 Eilola, K., Almroth-Rosell, E., and Meier, H. E. M.: Impact of saltwater inflows on phosphorus cycling and eutrophication in the Baltic Sea:
439 a 3D model study, *Tellus A*, <http://dx.doi.org/10.3402/tellusa.v66.23985>, 2014.

440 Flynn, K. J.: Ecological modelling in a sea of variable stoichiometry: Dysfunctionality and the legacy of Redfield and Monod, *Progress in
441 Oceanography*, 84, 52–65, doi:10.1016/j.pocean.2009.09.006, <http://dx.doi.org/10.1016/j.pocean.2009.09.006>, 2010.

442 Fransner, F., Gustafsson, E., Tedesco, L., Vichi, M., Hordoir, R., Roquet, F., Spilling, K., Kuznetsov, I., Eilola, K., Mörth, C., Humborg,
443 C., and Nylander, J.: Non-Redfieldian Dynamics Explain Seasonal pCO₂ Drawdown in the Gulf of Bothnia, *Journal of Geophysical
444 Research: Oceans*, 123, 166–188, doi:10.1002/2017JC013019, <https://agupubs.onlinelibrary.wiley.com/doi/abs/10.1002/2017JC013019>,
445 2018.

446 Graham, L. P.: Modeling runoff to the Baltic Sea, *Ambio*, 28, 328–334, 1999.

447 Granéli, E., Wallström, K., Larsson, U., Granéli, W., and Elmgren, R.: Nutrient limitation of primary production in the Baltic Sea Area,
448 *Ambio*, 19, 1990.

449 Grinsted, a., Moore, J. C., and Jevrejeva, S.: Application of the cross wavelet transform and wavelet coherence to geophysical time series,
450 *Nonlinear Processes in Geophysics*, 11, 561–566, doi:10.5194/npg-11-561-2004, <http://www.nonlin-processes-geophys.net/11/561/2004/>,
451 2004.

457 Gustafsson, B. G., Schenk, F., Blenckner, T., Eilola, K., Meier, H. E. M., Müller-Karulis, B., Neumann, T., Ruoho-Airola, T., Savchuk, O. P.,
458 and Zorita, E.: Reconstructing the development of baltic sea eutrophication 1850-2006, *Ambio*, 41, 534–548, doi:10.1007/s13280-012-
459 0318-x, 2012.

460 Hansson, D., Eriksson, C., Omstedt, A., and Chen, D.: Reconstruction of river runoff to the Baltic Sea, AD 1500-1995, *International Journal*
461 of *Climatology*, 31, 696–703, doi:10.1002/joc.2097, 2011.

462 HELCOM: Approaches and methods for eutrophication target setting in the Baltic Sea region., *Balt. Sea Env. Proc. No. 1*, 2012., 2012.

463 Jackett, D. R., McDougall, T. J., Feistel, R., Wright, D. G., and Griffies, S. M.: Algorithms for density, potential temperature, con-
464 servative temperature, and the freezing temperature of seawater, *Journal of Atmospheric and Oceanic Technology*, 23, 1709–1728,
465 doi:10.1175/JTECH1946.1, 2006.

466 Jakobsen, H. H. and Markager, S.: Carbon-to-chlorophyll ratio for phytoplankton in temperate coastal waters: Seasonal patterns and rela-
467 tionship to nutrients, *Limnol. Oceanogr.*, 61, 1853–1868, doi:10.1002/lno.10338, 2016.

468 Kahru, M., Elmgren, R., and Savchuk, O. P.: Changing seasonality of the Baltic Sea, *Biogeosciences*, 13, 1009–1018, doi:10.5194/bg-13-
469 1009-2016, 2016.

470 Lau, K. and Weng, H.: Climate signal detection using wavelet transform: How to make a time series sing, *Bulletin of the American Meteo-
471 rological Society*, 76, 2391–2402, doi:10.1175/1520-0477(1995)076<2391:csduwt>2.0.co;2, 1995.

472 Meier, H. E. M. and Kauker, F.: Modeling decadal variability of the Baltic Sea : 2 . Role of freshwater inflow and large-scale atmospheric
473 circulation for salinity, *Journal of Geophysical Research*, 108, 1–16, doi:10.1029/2003JC001799, 2003.

474 Meier, H. E. M., Döscher, R., and Faxén, T.: A multiprocessor coupled ice- ocean model for the Baltic Sea: application to the salt inflow.,
475 *Journal of geophysical research*, 108, doi:10.1029/2000JC000521, 2003.

476 Meier, H. E. M., Andersson, H. C., Arheimer, B., Blenckner, T., Chubarenko, B., Donnelly, C., Eilola, K., Gustafsson, B. G., Hansson, A.,
477 Havenhand, J., Höglund, A., Kuznetsov, I., MacKenzie, B. R., Müller-Karulis, B., Neumann, T., Niiranen, S., Piwowarczyk, J., Raudsepp,
478 U., Reckermann, M., Ruoho-Airola, T., Savchuk, O. P., Schenk, F., Schimanke, S., Väli, G., Weslawski, J.-M., and Zorita, E.: Comparing
479 reconstructed past variations and future projections of the Baltic Sea ecosystem—first results from multi-model ensemble simulations,
480 *Environmental Research Letters*, 7, 034 005, doi:10.1088/1748-9326/7/3/034005, 2012.

481 Meier, H. E. M., Höglund, A., Eilola, K., and Almroth-Rosell, E.: Impact of accelerated future global mean sea level rise on hypoxia in the
482 Baltic Sea, *Climate Dynamics*, pp. 1–10, doi:10.1007/s00382-016-3333-y, 2016.

483 Meier, H. E. M., Väli, G., Naumann, M., Eilola, K., and Frauen, C.: Recently accelerated oxygen consumption rates amplify deoxygenation
484 in the Baltic Sea., *Journal of Geophysical Research*, in press.

485 Menden-Deuer, S. and Lessard, E. J.: Carbon to volume relationships for dinoflagellates, diatoms, and other protist plankton, *American*
486 *Society of Limnology and Oceanography*, 3, doi:10.4319/lo.2000.45.3.0569, 2000.

487 Parker, R. A.: Dynamic models for ammonium inhibition of nitrate uptake by phytoplankton, *Ecological Modelling*, 66, 113–120,
488 doi:10.1016/0304-3800(93)90042-Q, 1993.

489 Rakko, A. and Seppälä, J.: Effect of salinity on the growth rate and nutrient stoichiometry of two Baltic Sea filamentous cyanobacterial
490 species., *Estonian Journal of Ecology*, 63, 55–70, doi:10.3176/eco.2014.2.01, 2014.

491 Redfield, A. C.: The biological control of chemical factors in the environment, *American Scientist*, 46, 205–221, doi:10.5194/bg-11-1599-
492 2014, 1958.

493 Ruoho-Airola, T., Eilola, K., Savchuk, O. P., Parviainen, M., and Tarvainen, V.: Atmospheric nutrient input to the baltic sea from 1850 to
494 2006: A reconstruction from modeling results and historical data, *Ambio*, 41, 549–557, doi:10.1007/s13280-012-0319-9, 2012.

495 Savchuk, O. P.: Large-Scale Dynamics of Hypoxia in the Baltic Sea, in: Chemical structure of pelagic redox interfaces: Observation and
496 modeling, Hdb Env Chem, edited by Yakushev, E. V., pp. 137–160, Springer-Verlag, Berlin Heidelberg, doi:10.1007/698_2010_53, 2010.

497 Savchuk, O. P., Wulff, F., Hille, S., Humborg, C., and Pollehnne, F.: The Baltic Sea a century ago — a reconstruction from model simulations,
498 verified by observations, *Journal of Marine Systems*, 74, 485–494, doi:10.1016/j.jmarsys.2008.03.008, <http://linkinghub.elsevier.com/retrieve/pii/S0924796308000572>, 2008.

500 Savchuk, O. P., Gustafsson, B. G., Rodríguez, M., Sokolov, A. V., and Wulff, F. V.: External nutrient loads to the Baltic Sea , 1970-2006,
501 2012.

502 Schernewski, G. and Neumann, T.: The trophic state of the Baltic Sea a century ago: a model simulation study, *Journal of marine systems*,
503 53, 109–124, doi:<https://doi.org/10.1016/j.jmarsys.2004.03.007>, 2004.

504 Schimanke, S. and Meier, H.: Decadal to centennial variability of salinity in the Baltic Sea, *Journal of Climate*, pp. JCLI-D-15-0443.1,
505 doi:10.1175/JCLI-D-15-0443.1, <http://journals.ametsoc.org/doi/10.1175/JCLI-D-15-0443.1>, 2016.

506 Tamminen, T. and Andersen, T.: Seasonal phytoplankton nutrient limitation patterns as revealed by bioassays over Baltic Sea gradients of
507 salinity and eutrophication, *Marine Ecology Progress Series*, 340, 121–138, doi:10.3354/meps340121, 2007.

508 Torrence, C. and Compo, G. P.: A practical guide to wavelet analysis, *Bull. Amer. Meteor. Soc.*, pp. 61–78, 1998.

509 Tyrrell, T.: The relative influences of nitrogen and phosphorus on oceanic primary production, *Nature*, 400, 525–531, 1999.

510 Vahtera, E., Conley, D. J., Gustafsson, B. G., Kuosa, H., Pitkanen, H., Savchuk, O. P., Tamminen, T., Viitasalo, M., Wasmund, N., and Wulff,
511 F.: Internal Ecosystem Feedbacks Enhance Nitrogen-fixing Cyanobacteria., *Ambio*, 36, 186–193, 2007.

512 Winder, M. and Cloern, J. E.: The annual cycles of phytoplankton biomass., *Philosophical transactions of the Royal Society of London.*
513 Series B, Biological sciences

514 365, 3215–26, doi:10.1098/rstb.2010.0125, <http://rstb.royalsocietypublishing.org/content/365/1555/3215>, 2010.

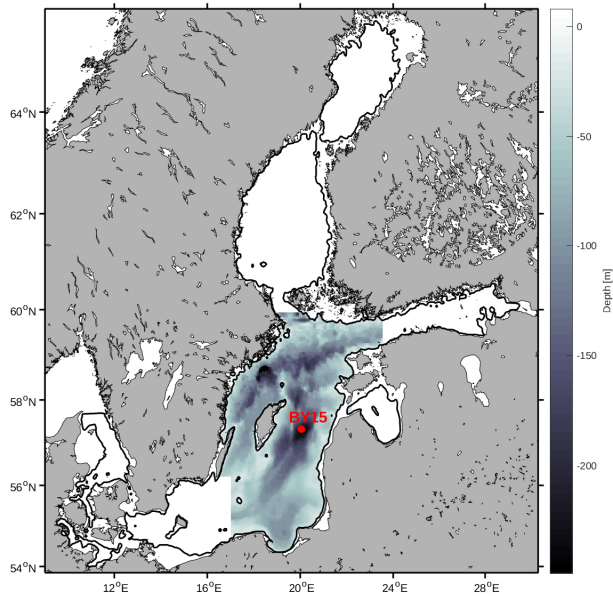


Figure 1. Study area. The grey scale represents depth in m. [The red dot represents the monitoring station BY15](#)

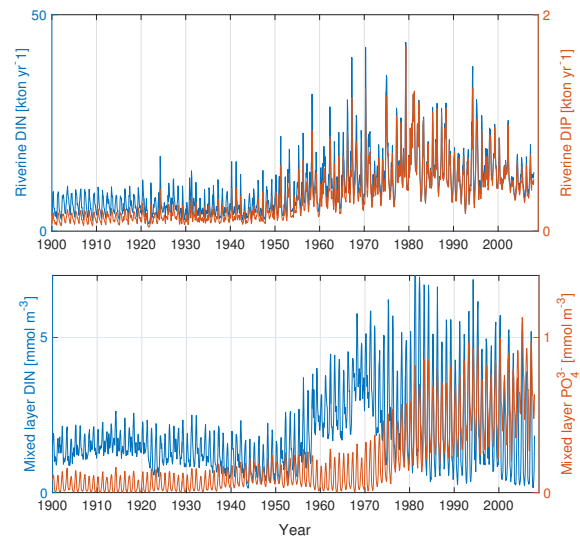


Figure 2. The top panel shows riverine DIN (blue) and phosphate DIP (red) loads [to the Baltic proper as defined in Fig. 1](#). The bottom panel shows mixed layer DIN (blue) and [mixed layer](#) phosphate (red) [averaged over the study area](#).

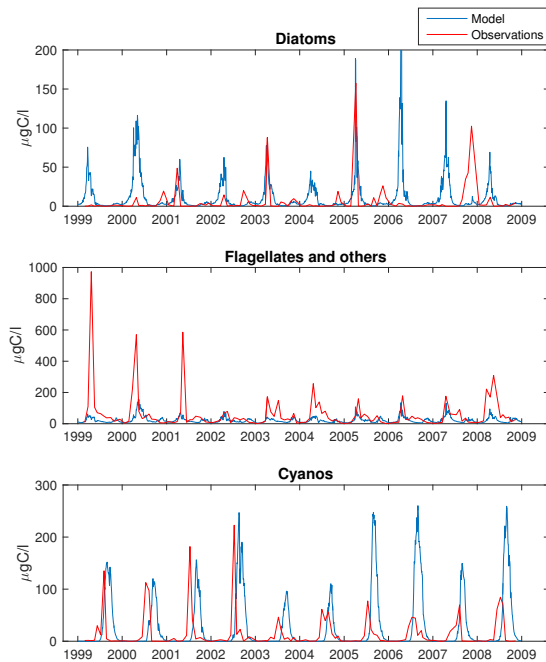


Figure 3. Simulated (blue) and observed (red) biomass of diatoms (top), flagellates and others (middle) and cyanobacteria (bottom) at BY15.

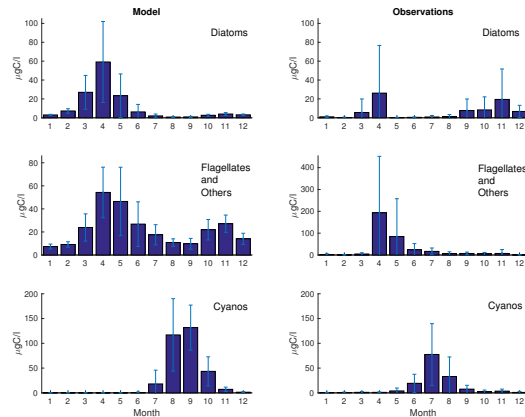


Figure 4. Monthly means of simulated (left) and observed (right) diatoms (top), flagellates and others (middle) and cyanobacteria (bottom) at BY15. Standard deviations are shown as errorbars.

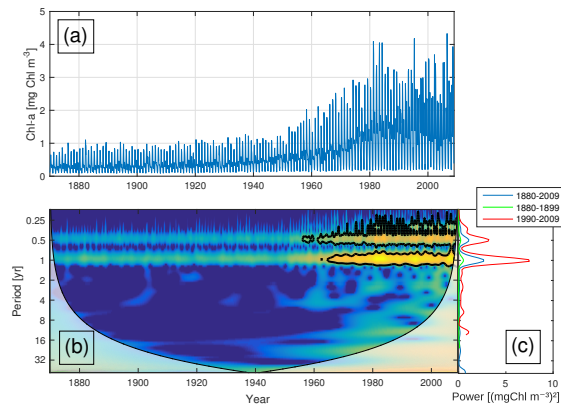


Figure 5. Time-series of phytoplankton biomass (a) together with the corresponding wavelet power spectrum (b) and global wavelet spectrum (c). More yellow means more power. The black curves in (b) represent the 95% confidence level relative to red noise. The white areas in (b) represent the cone of influence in which the results are impacted by edge-effects and are therefore not shown. The different lines in (c) represent the global spectrum 1880-2009 (blue), 1880-1899 (green), 1990-2009 (red).

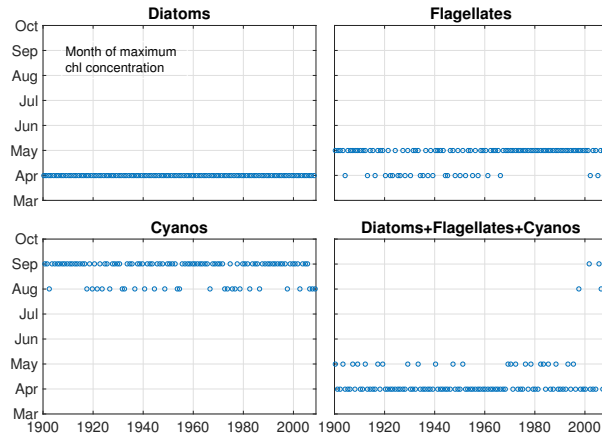


Figure 6. The month of maximum ~~concentration~~ ~~biomass~~ of diatoms, flagellates and cyanobacteria as well as their sum.

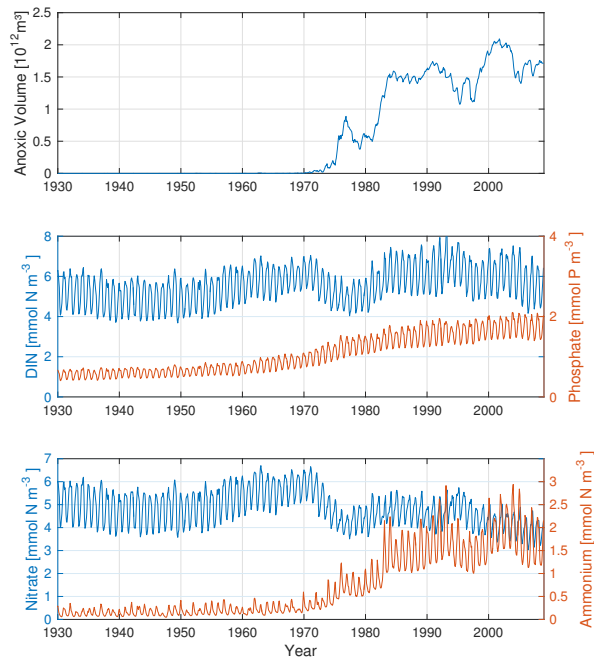


Figure 7. Time-series of anoxic volume (top), below mixed layer concentrations of DIN (nitrate + ammonium, blue) and phosphate (red) (middle) and nitrate (blue) and ammonium (red) (bottom) averaged over the Baltic proper.

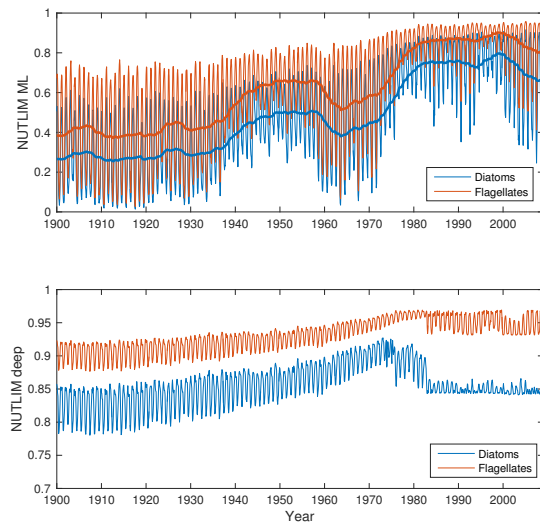


Figure 8. Time-series of nutrient limitation in the mixed layer (top) and below (bottom) for diatoms (blue) and flagellates (red). The thicker lines in the top panel show the 5yr-5-year moving average.

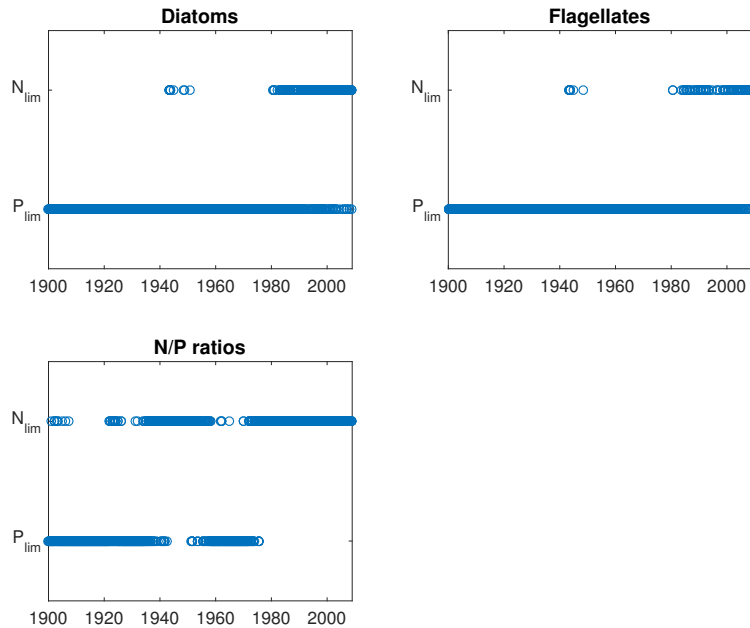


Figure 9. Nitrogen Mixed layer nitrogen or phosphate limitation as function of time **in the mixed layer (upper panels) and in the deep water (lower panels)** of for diatoms (upper left panels) and flagellates (upper right panels) as calculated through Eq. (2) where N limitation occurs when $N_{\text{LIM}} < P_{\text{LIM}}$. The bottom panel shows nutrient limitation as calculated through N/P ratios, where N limitation occurs when $N/P < 16$. Note that simultaneous N and P limitation is not possible although the size of the rings **in the figures** gives this appearance.

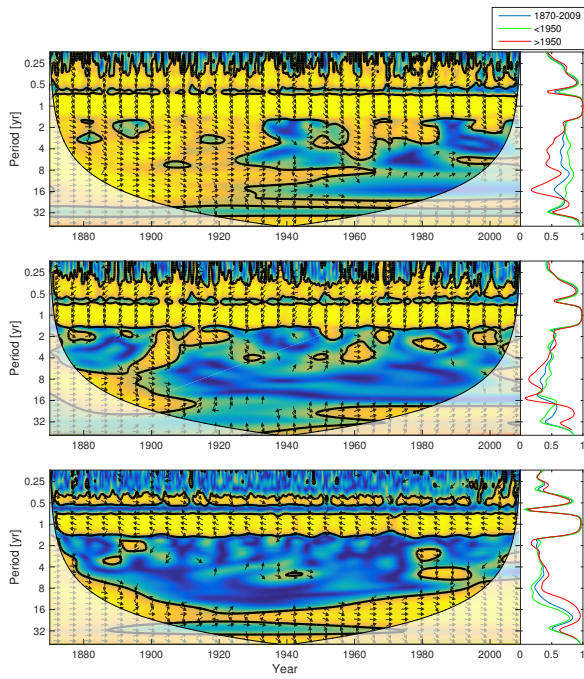


Figure 10. Wavelet coherence between mixed layer phosphate concentration and diatoms (top), flagellates (middle) and cyanobacteria (bottom). More yellow means more coherence. The arrows indicate the phase lag. When pointing to the right the two time-series are in phase and when pointing in the opposite direction anti-phase. The right panels show the coherence averaged over the whole period (blue) and before (green) and after (red) 1950.

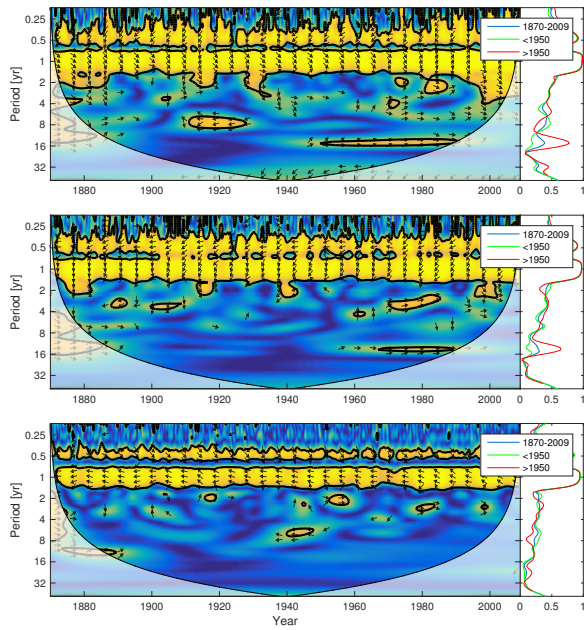


Figure 11. Wavelet coherence between mixed layer DIN concentration and diatoms (top), flagellates (middle) and cyanobacteria (bottom).

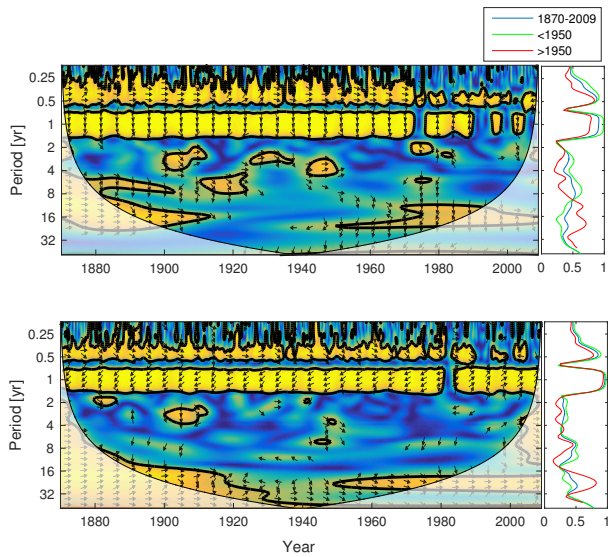


Figure 12. Wavelet coherence between deep water NUTLIM and diatoms (top), flagellates (middle)

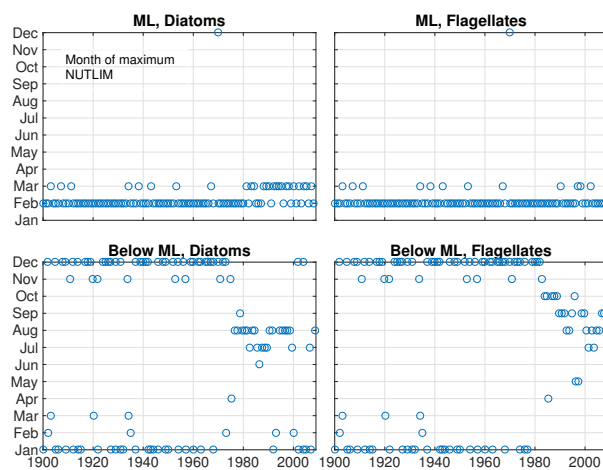


Figure 13. The month of maximum NUTLIM for diatoms (left) and flagellates (right) in the mixed layer (top) and below (bottom).

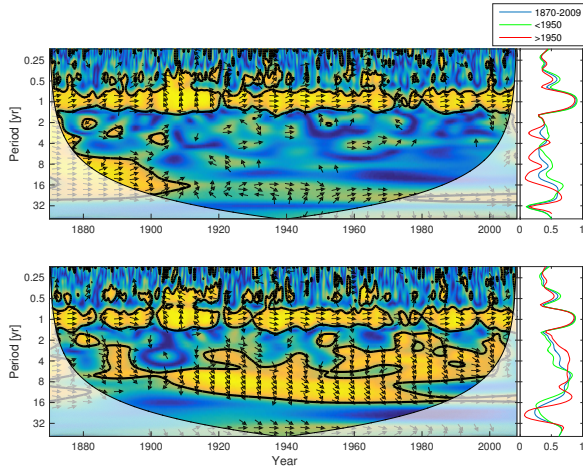


Figure 14. Wavelet coherence between riverine phosphate and mixed layer phosphate concentration (top) and riverine DIN and mixed layer DIN concentration (bottom). The arrows indicates the phase lag. When pointing to the right the two time-series are in phase and when pointing in the opposite direction anti-phase. The right panels show the averaged coherence for the whole period (blue) and before (green) and after (red) 1950.

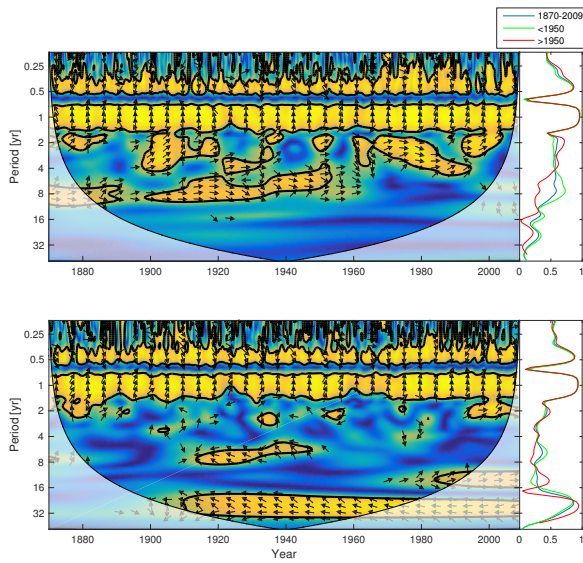


Figure 15. Wavelet coherence between mixed layer salinity and phosphate concentration (top) and mixed layer salinity and nitrate concentration (bottom). The right panels show the averaged coherence spectrum.

515 2-yr moving average of mixed layer temperature (top) and mixed layer depth (bottom).

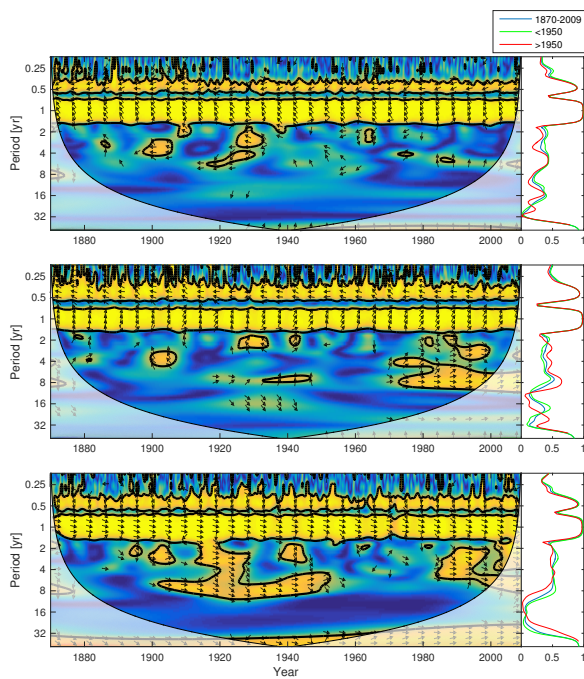


Figure 16. Wavelet coherence between mixed layer temperature and diatoms (top), flagellates (middle) and cyanobacteria (bottom).

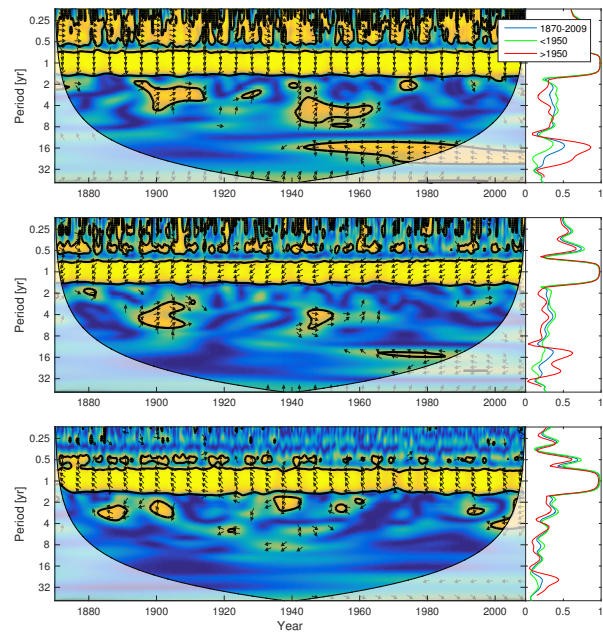


Figure 17. Wavelet coherence between mixed layer depth and diatoms (top), flagellates (middle) and cyanobacteria (bottom).